

ELECTROMAGNETISM, OPTICS, ACOUSTICS, HEAT TRANSFER, CLASSICAL MECHANICS, AND FLUID DYNAMICS

Different supercontinuum generation processes in photonic crystal fibers pumped with a 1064-nm picosecond pulse

To cite this article: Chen Hong-Wei *et al* 2013 *Chinese Phys. B* **22** 084205

View the [article online](#) for updates and enhancements.

You may also like

- [Broadband infrared supercontinuum generation in a soft-glass photonic crystal fiber pumped with a sub-picosecond Er-doped fiber laser mode-locked by a graphene saturable absorber](#)
Ryszard Buczynski, Grzegorz Sobon, Jaroslaw Sotor *et al*.
- [Intermodal dispersive waves and soliton collision during multimode supercontinuum generation in chalcogenide glass fiber](#)
Dengke Xing, Jiangyong He, Pan Wang *et al*.
- [Quantitative evaluation of the supercontinuum laser eye dazzling effect: *in vivo* experimental research](#)
Qiong Ma, Yingwei Fan and Hongxiang Kang

Different supercontinuum generation processes in photonic crystal fibers pumped with a 1064-nm picosecond pulse*

Chen Hong-Wei(谔鸿伟), Jin Ai-Jun(靳爱军), Chen Sheng-Ping(陈胜平),
Hou Jing(侯静)[†], and Lu Qi-Sheng(陆启生)

College of Optoelectronic Science and Engineering, National University of Defense Technology, Changsha 410073, China

(Received 13 January 2013; revised manuscript received 2 February 2013)

Picosecond pulse pumped supercontinuum generation in photonic crystal fiber is investigated by performing a series of comparative experiments. The main purpose is to investigate the supercontinuum generation processes excited by a given pump source through the experimental study of some specific fibers. A 20-W all-fiber picosecond master oscillator-power amplifier (MOPA) laser is used to pump three different kinds of photonic crystal fibers for supercontinuum generation. Three diverse supercontinuum formation processes are observed to correspond to photonic crystal fibers with distinct dispersion properties. The experimental results are consistent with the relevant theoretical results. Based on the above analyses, a watt-level broadband white light supercontinuum source spanning from 500 nm to beyond 1700 nm is demonstrated by using a picosecond fiber laser in combination with the matched photonic crystal fiber. The limitation of the group velocity matching curve of the photonic crystal fiber is also discussed in the paper.

Keywords: picosecond pulse, photonic crystal fiber, nonlinear fiber optics, supercontinuum generation

PACS: 42.55.Wd, 42.65.-K, 42.65.Tg

DOI: 10.1088/1674-1056/22/8/084205

1. Introduction

Supercontinuum (SC) generation in photonic crystal fiber (PCF) is a very hot research topic, and quite a number of theoretic and experimental investigations have been reported in recent years.^[1–3] The underlying mechanisms of SC generation are now well known.^[4,5] When a pump laser with defined initial characteristics propagates through a length of fiber, the nonlinear processes in an optical fiber occur. The main nonlinear effects involved in the SC generation process include self-phase modulation (SPM), four-wave-mixing (FWM) or modulation instability (MI), Raman scattering, and the soliton related effects (soliton formation, soliton propagation and break-up, soliton self-frequency shift (SSFS), dispersive wave generation, soliton or dispersive wave trapping). The parameters of the input pump laser and the properties of the fiber itself determine what kind of nonlinear effect would take place and the form of the output. Different conditions would result in distinct SC generation processes. In order to control the SC generation progress, not only the parameters of the pump source (pump wavelengths, pulse duration, and the pump power level) but also the properties of fiber (the material of fiber, geometry parameters) should be carefully considered. The conjunction of an optimized pump source with the matched fiber could yield the desired SC. Theoretically there are countless lasers that could be used as the pump sources. However, the available pump lasers are limited in practice, especially for the purpose of engineering. While the properties of the fiber, especially

the dispersion property, also have notable influence on the SC generation progress. Thus designing a fiber to match a given pump source is more like a feasible solution.^[6]

Up to now, femtosecond, picosecond or even the continuous wave (CW) lasers have been used as the SC pumps. The femtosecond laser-pumped SC usually exhibits a broadband continuum range due to the high pulse peak power and short pulse duration, while the system of the femtosecond pump source itself is complex.^[7] It is also hard to configurate a femtosecond pumped SC source with an all-fiber architecture.^[8] The CW-pumped SC could obtain a high average power and high spectral power density output.^[9] However, compared with the pulse-pumped SC, the CW-pumped SC has a relatively narrow spectral range. In fact, the picosecond fiber laser is an ideal SC pump source. On the one hand its high pulse peak power is helpful for exciting the nonlinear effects;^[10–12] on the other hand it is feasible to form a high power all-fiber picosecond laser,^[13] then to form an SC source with an all-fiber architecture.^[14]

In our previous work, with the mode-locked technology and MOPA chain, we demonstrated a high power all-fiber picosecond laser at 1064 nm, which was suitable for serving as the SC pump source.^[15] We also presented high power SC generation in PCF with the self-made picosecond fiber lasers.^[16,17] These SC generation processes were similar in those experiments, for the PCFs used were of the same kind. Another issue is that the visible SC generation is limited due to the property of the used PCF. The main purpose of this

*Project supported by the State Key Program of the National Natural Science Foundation of China (Grant No. 61235008) and the Postgraduate Innovation Foundation of National University of Defense Technology, China (Grant No. B110704).

[†]Corresponding author. E-mail: houjing25@sina.com

paper is to investigate the SC generation processes in different photonic crystal fibers pumped by a given pump source. Here, we investigate the 1064-nm picosecond pulse-pumped SC generations in three different kinds of photonic crystal fibers, which possess distinct dispersion properties. Three diverse SC formation processes are observed, though the same pump source is used in the three cases. As a practical application, a watt-level broadband picosecond pulse-pumped white light SC source is demonstrated with the matched photonic crystal fiber.

2. Basic theory and experimental setup

The typical SC generation theory is that^[5] if the short pulse (subpicosecond) pumps in anomalous GVD regime of the PCF, the spectral broadening would arise from soliton-related dynamics. The pump pulse is generally considered to be high-order solitons, owing to its high peak power. Then it breaks up into a series of distinct fundamental soliton components due to the perturbations. Continued propagation of the solitons could result in a continuous shift toward longer wavelengths through the Raman self-scattering. The red-shifts of these fundamental solitons are associated with the generations of blue-shifted dispersive wave spectral components. For pump pulses with longer durations (picosecond, nanosecond, and CW), the characteristic length of soliton fission becomes very long. So the soliton fission process becomes less important during initial propagation. Instead, MI occurs on the same length scale regardless of the pulse duration. The initial MI dynamics leads to the temporal breakup of the pump pulse into a large number of subpulses. Further spectral broad-

ening arises essentially in the same way as that in the case with using short pump pulses. For the case of pumping in the normal GVD regime, the spectral broadening dynamics for the subpicosecond pulse arises from the interaction between the self-phase modulation and the normal GVD of the fiber, with shorter pulses inducing greater nonlinear broadening; for longer pulses, significant initial spectral broadening can develop from four-wave mixing or Raman scattering. In this case, once the spectral broadening begins to overlap with the zero dispersion wavelength (ZDW), soliton dynamics then play an increasingly important role as well.

In our experiments, three different kinds of index guiding photonic crystal fibers are used as the SC generation media, labeled as PCF 1, PCF 2, and PCF 3 respectively. PCF 1 and PCF 3 are self-made fibers, the PCF 2 is a commercial fiber. The main parameters of the three PCFs are listed in Table 1. The geometric shapes of the three PCFs are similar while the air-hole diameters and the pitches are different, corresponding to different fiber properties. Two picosecond fiber lasers with different average output powers and different pulse repetition rates are used as the pump sources. One is a 20-W all-fiber picosecond MOPA laser, which delivers 14-ps pulse with 480-MHz repetition rate at 1064 nm. The other one outputs 4.5-W picosecond pulse laser with a pulse duration of ~ 14 ps and a pulse repetition rate of 60 MHz. The output pigtail fibers of the two pumps are the same kind double cladding fibers (DCFs) each with 15 μm /130 μm core/cladding diameter. The output pigtail fiber is directly spliced with the PCFs to form an all-fiber configuration. The experimental setup is schematically shown in Fig. 1.

Table 1. Parameters of three different PCFs.

	PCF 1	PCF 2	PCF 3
Geometry shape	Five hexagonal rings of circular air-holes	Six hexagonal rings of circular air-holes	Five hexagonal rings of circular air-holes
Hole diameter/ μm	3.5	1.6	2.0
Pitch/ μm	5.4	3.2	3.3
Core diameter/ μm	7.3	4.8	4.6
Zero dispersion wavelength/nm	~ 1120	~ 1033	~ 1012
PCF length/m	40	20	20

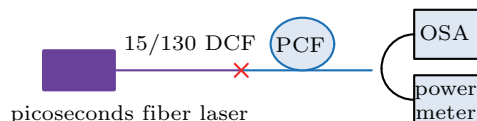


Fig. 1. (color online) Experimental setup.

3. Results and discussion

The experiments in four comparative cases are carried out and the main parameters of the generated SC in different cases are listed in Table 2. First we use the 20-W picosecond fiber

laser as the pump source and observe the output property from the three different kinds of PCFs, corresponding to case 1, case 2, and case 3 in Table 2. The output properties of the SC sources are observed directly from the output end of the PCF. The output power is measured with a coherent EPM 2000 power meter and the output is coupled into an optical spectrum analyzer (OSA) via an intermediate fiber for spectral analysis (Agilent 86142B with a resolution bandwidth of 5 nm). Figure 2 shows the output power properties and the output spectrum evolutions versus SC power in the three cases.

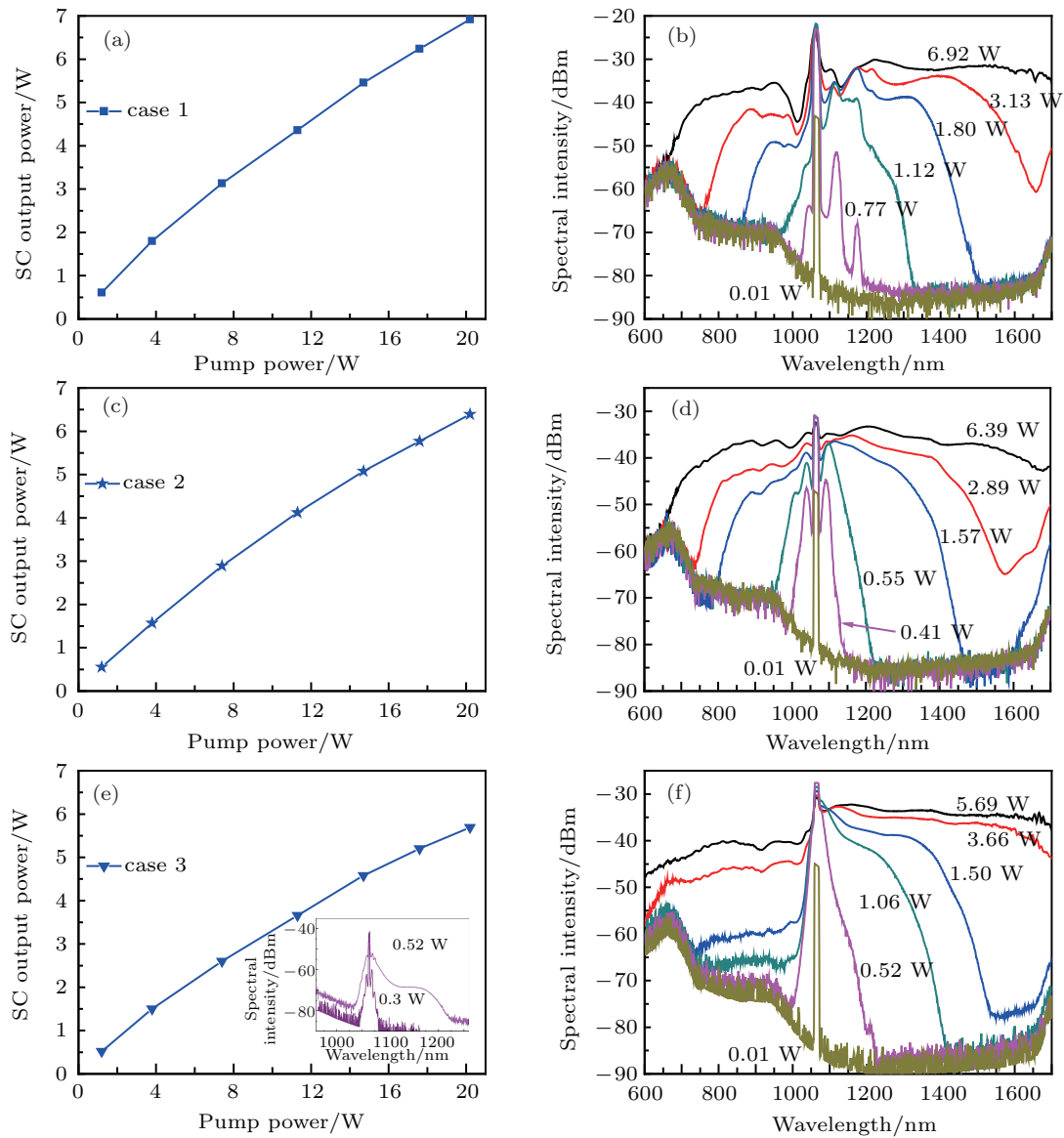


Fig. 2. (color online) Output power properties and the output spectrum evolutions versus SC power for case 1 (panels (a) and (b)), case 2 (panels (c) and (d)), and case 3 (panels (e) and (f)).

Table 2. Parameters of the generated SC in different cases.

	Case 1*	Case 2	Case 3	Case 4
PCF category	PCF 1	PCF 2	PCF 3	PCF 3
Pump power/W	20	20	20	4.5
Pulse duration/ps	14	14	14	14
Pulse repetition rate/MHz	480	480	480	60
Pump wavelength/nm	1064	1064	1064	1064
SC power/W	6.9	6.39	5.69	1.64
SC range/nm	blue side	660	< 600	500
	red side	> 1700	> 1700	> 1700
Initial nonlinear effects	SRS	MI	MI + SSFS	MI + SSFS

* Case 1 has been reported in our previous paper, readers can refer to Ref. [16] for more details

For case 1, 6.69-W SC is obtained under the full pump power and the optical–optical conversion efficiency is 34% (see Fig. 2(a)). Figure 2(b) shows the spectrum variation with SC output power. As the zero dispersion wavelength (ZDW) of PCF 1 is 1117 nm, the 1064-nm pump is in the normal

dispersion region of PCF. Two spectral peaks are present at about 1120 nm and 1175 nm, when the SC output power is low (less than 0.77 W). The frequency shift of every two closer peaks is about ~ 13 THz, corresponding to the Raman frequency shift in silicon fiber, which indicates that stimulated Raman scattering (SRS) dominates the initial step of SC generation. With output power increasing to 1.12 W, the spectrum becomes a continuum and the Raman peaks are submerged in the SC. Most of the SC components are present on the red side of the 1064-nm pump wavelength, and the SC has passed over the ZDW of PCF. When the output power increases to a higher power level (1.80 W), the blue side SC appears at about 900 nm due to the dispersion wave generation. This result indicates that the soliton mechanism occurs at this stage of SC generation. Then the SC broadens to both sides with nm, more details are not observed for lack of available OSA. The flatness of the final output spectrum is not so considerable

and some spectral gaps are observed at about 1010 nm and 1127 nm.

For case 2, the output power property is shown in Fig. 2(c). The 6.39-W SC is obtained under the full pump power, and the optical–optical conversion efficiency is 32%. The plots of output spectrum versus SC output power are shown in Fig. 2(d). In this case, the ZDW of PCF 2 is 1033 nm, so the 1064-nm pump is in the anomalous dispersion region of PCF. As shown in Fig. 2(d), the SC broadening process starts with the generation of a Stokes (~ 1090 nm) and an anti-Stokes (~ 1039 nm) component around the pump wavelength. The symmetric arrangement of the frequency pairs demonstrates that MI (equivalently, the generation of FWM parametric sidebands) is responsible for the spectral broadening at the beginning of SC generation. With the increase of output power, the output spectrum extends to both short and long wavelengths sides. As a result, an SC spanning from 660 nm to beyond 1700 nm is observed. The spectral flatness of the SC is improved and no obvious spectral gaps are observed in case 2 compared with those in case 1.

For case 3, as shown in Fig. 2(e), 5.69-W SC is obtained under the full pump power, and the optical–optical conversion efficiency is 28.4%. Note that the ZDW of the PCF 3 is 1012 nm, the 1064-nm picosecond pump wavelength is also in the anomalous dispersion region. The output spectrum evolutions of the SC source with different output powers are shown in the inset of Figs. 2(e) and 2(f). As shown in the inset of Fig. 2(e), several symmetric frequency pairs are observed around the 1064-nm pump wavelength when the SC output power is low (0.3 W), which indicates the initial output spectrum broadens by means of MI too. While the frequency shifts of the generated spectral side bands are relatively narrow compared with those in case 2. With output power increasing to 0.52 W, the output spectrum becomes unsymmetrical and most of spectral components continually extend to the long wavelength range (see Fig. 2(f)). The SSFS dominates the spectral broadening process at this stage. Increasing the output power to 1.06 W, the spectral components located at around 900 nm are observed. Then the SC quickly broadens to both sides with the increase of output power. The output spectrum at full output power is displayed in Fig. 2(f) (the top curve). The SC ranges from 600 nm to 1700 nm (spectrum components below 600 nm and beyond 1700 nm are not observed due to the limitation of the OSA). In this case, the spectral broadening on the short wavelength side is obviously enhanced. We can observe the white light radiation with naked eyes.

The power loss between the delivery DCF and the PCF is mainly caused by the mode field diameter (MFD) mismatch. As suggested in Ref. [18], when the interface fusion splicing technique is used to splice a PCF with other fiber, the splicing loss induced from the MFD mismatch can be estimated by the

following equation

$$\alpha = -20 \cdot \lg \left(\frac{2\omega_{\text{PCF}} \cdot \omega_{\text{DCF}}}{\omega_{\text{PCF}}^2 + \omega_{\text{DCF}}^2} \right), \quad (1)$$

where α is the splice loss, ω_{PCF} and ω_{DCF} are the mode-field diameters (MFDs) of the PCF and the DCF, respectively. The ω_{DCF} (~ 16 μm) is uniform in our experiment, the ω_{PCF} is gradually reduced from PCF 1 to PCF 2 to PCF 3. According to Eq. (1), the splice loss will be increased when the ω_{PCF} is reduced from PCF 1 to PCF 2 to PCF 3. This is also verified by our experimental experience.

For a given PCF, a high splice loss means that the effective pump power is relatively low. Thus, there will arise two influences on the SC generation: the output power will be dropped off and the spectral broadband will be shrunk. It should be noticed that the above discussion is based on different effective pump powers for a fixed PCF. In the three comparative experiments, the SC output power decreases from case 1 to case 3 at the same pump power level. It is possibly because 1) with the core diameter of the PCF decreasing from case 1 to case 3, the splice loss between the DCF and PCF increases though the low current multi-discharge method is adopted to minimize the splice loss in those experiments; 2) the nonlinear broadening processes in the three cases are different, so the quantum defects from the pump photons to the generated photons are different. The SC in case 3 is broadest, then the quantum defect should be highest correspondingly.

However, the most interesting thing is that three diverse SC formation processes have been observed in those experiments. Though the splice loss between the DCF and PCF 3 should be largest according to Eq. (1), the SC in case 3 is broadest. The SC pump in our experiments is the same one, so what SC generation process will be excited is determined by the kind of the PCF. The GVD curves of the three PCFs are shown in Fig. 3. In case 1, the 1064-nm pump wavelength is in the normal dispersive region of PCF 1 but a little far from the ZDW, so the parametric sidebands are too much detuned from the pump. Thus SRS dominates the initial step of SC generation. Once this broadening begins to overlap with the ZDW, soliton effects can again contribute to the overall dynamics. In cases 2 and 3, the 1064-nm pump wavelength is located in the anomalous GVD regime. While the 1064-nm pump wavelength is in the vicinity of the ZDW of PCF 2, the phase-match condition, which is required in the parametric progress, can be easily satisfied in case 2. So MI dominates the initial pulse propagation. Then soliton dynamics plays an important role in the following stages. In case 3, the ZDW of PCF 3 is a little far from the 1064-nm pump wavelength. The initial MI dynamics does not generate sufficient bandwidth to efficiently seed dispersive wave transfer into the normal GVD regime. However, the MI also leads to the temporal breakup of the pump pulse

into a large number of subpulses. Once solitons are formed, SSFS takes place, resulting in widening the input spectrum to longer wavelengths on the order of several tens or hundreds of nanometers. Simultaneously, these soliton pulses shed energy to matched dispersive waves located on the short-wavelength side of the pump. Because the initial SSFS process is in favor of generating the matched dispersive wave on the short wavelength side, the PCF 3 could enhance the spectral broadening on the short wavelength side. The SPM and cross-phase modulation (XPM) could also help to smoothen the output spectra in cases 2 and 3. The SC generation processes in our experiments are consistent with the typical SC generation theory.

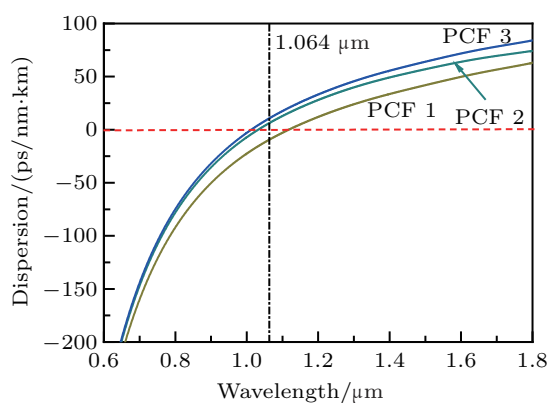


Fig. 3. (color online) The GVD curves of the three PCFs.

Based on the above analysis, for the 1064-nm picosecond fiber laser, the self-made PCF 3 rather than the commercially available PCF 2 is more suitable for the broadband SC generation. In order to verify this fact, we build a watt-level broadband white light SC source with self-made picosecond pump laser and PCF 3, corresponding to case 4 in Table 2. A 1064-nm picosecond pulse laser with 4.5-W output is used as the pump source and the pulse repetition rate is reduced to 60 MHz to maintain a high pulse peak power. We also optimize the splice loss between the delivery DCF and the PCF using the controlled air-hole collapse technique.^[19] The 1.64-W SC is obtained under the full pump power, and the optical-optical conversion efficiency is 36.4%. The output is coupled into an Ando OSA via an intermediate fiber for spectral analysis (with a resolution bandwidth of 1 nm). The output spectrum evolution is shown in Fig. 4. The SC generation process is very similar to that in case 3, and a broadband SC with a spectral range from 500 nm to beyond 1700 nm is obtained. The inset in Fig. 4 shows the grating-separated SC output light.

It should be noted that the blue side of the SC generated in PCF 3 is limited to about 500 nm, but the SC source with blue light is more desired in the practical applications. Though the distinct initial processes appear in different PCFs, soliton-related effects would dominate the spectral broadening at the advance stage of the SC generation. The generated Raman

soliton and the group velocity matched dispersive waves can couple through XPM to generate additional frequency components that increase the overall bandwidth.^[5] In other words, the trapped dispersive waves or trapped solitons, based on the group velocity matching, principally determine the overall spectral range of the SC. The group velocity curves of the three PCFs are shown in Fig. 5. As shown in Fig. 5, in order to extend the short wavelength side of the SC to 500 nm, the long wavelength side of the SC should broaden to be over 2000 nm. The group velocity matching curve of PCF 3 looks like the best one for the short wavelength SC generation. But the group velocity matching curve also indicates that the short wavelength of the SC generated from PCF 3 is limited to about 500 nm, which has been verified by our experimental results. In order to increase the blue-shift of the generated SC, not only the dispersive property but also the suitable group velocity matching curve should be considered when a PCF is designed.

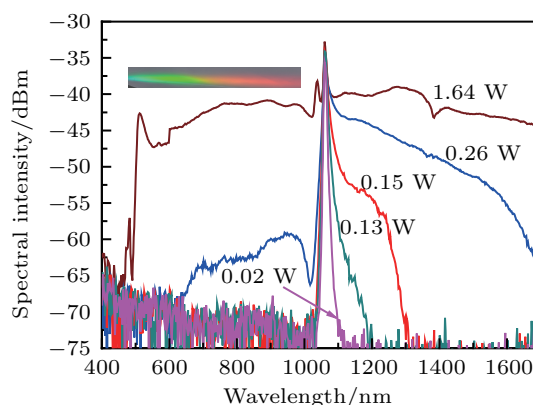


Fig. 4. (color online) Output spectrum evolutions versus the SC power in case 4. The inset shows the grating separated SC light.

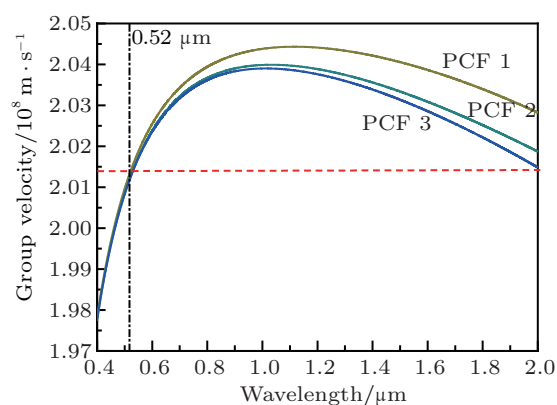


Fig. 5. (color online) Curves of group velocity versus wavelength for the three PCFs.

4. Conclusions

In order to investigate the SC generation processes excited by a given pump source, three different kinds of photonic crystal fibers with distinct dispersion properties are tested in our experiments. A 20-W all-fiber picosecond MOPA laser

is used to pump the three different kinds of photonic crystal fibers for SC generation. Three diverse SC formation processes are observed. The dispersion properties of the PCF would have a notable influence on the SC generation progress for the given pump source. A watt-level broadband white light SC source spanning from 500 nm to beyond 1700 nm is demonstrated with a 1064-nm picosecond fiber laser in combination with the matched PCF 3. The group velocity matching curve of the PCF 3 is still less favorable for the short wavelengths generation. According to the experimental results, we could obtain some experiential references for designing a suitable PCF to match a given pump source. How to optimize a PCF for a 1064-nm picosecond pump laser will be studied in a future work.

References

- [1] Ranka J K, Windeler R S and Stentz A J 2000 *Opt. Lett.* **25** 25
- [2] Dudley J M and Taylor J R 2010 *Supercontinuum Generation in Photonic Crystal Fibers* (New York: Cambridge University Press)
- [3] Wang X Y, Li S G, Liu S, Yin G B and Li J S 2012 *Chin. Phys. B* **21** 054220
- [4] Dudley J M, Genty G and Coen S 2006 *Rev. Mod. Phys.* **78** 1135
- [5] Genty G, Coen S and Dudley J M 2007 *J. Opt. Soc. Am. B* **24** 1771
- [6] Stone J M and Knight J C 2012 *Opt. Fiber Technol.* **18** 315
- [7] Yuan J H, Sang X Z, Yu C X, Xin X J, Shen X W, Zhang J L, Zhou G Y, Li S G and Hou L T 2011 *Chin. Phys. B* **20** 054210
- [8] Fang X H, Wang Q Y, Liu J J, Liu B W, Li Y F, Chai L and Hu M L 2010 *Chin. J. Lasers* **37** 1585
- [9] Labat D, Mélin G, Mussot A, Fleureau A, Galkovsky L, Lempereur S and Kudlinski A 2011 *IEEE Photon. J.* **3** 815
- [10] Pan E M, Ruan S C, Guo C Y, Wang Y C and Wei H F 2010 *Chin. Phys. Lett.* **27** 100702
- [11] Chen K K, Alam S U, Price J H V, Hayes J R, Lin D J, Malinowski A, Codemard C, Ghosh D, Pal M, Bhadra S K and Richardson D J 2010 *Opt. Express* **18** 5426
- [12] Zhu X, Zhang X B, Chen X, Peng J G, Dai N L and Li J Y 2012 *Chin. Phys. Lett.* **29** 124210
- [13] Chen S P, Chen H W, Hou J and Liu Z J 2009 *Opt. Express* **17** 24008
- [14] Hu X, Zhang W, Yang Z, Wang Y, Zhao W, Li X, Wang H, Li C and Shen D 2011 *Opt. Lett.* **36** 2659
- [15] Chen H W, Lei Y, Chen S P, Hou J and Lu Q S 2012 *Appl. Phys. B* **109** 233
- [16] Chen H W, Chen S P and Hou J 2011 *Laser Phys.* **21** 191
- [17] Chen H W, Chen S P, Wang J H, Chen Z L and Hou J 2011 *Opt. Commun.* **248** 5484
- [18] Xiao L M, Demokan M S, Jin W, Wang Y and Zhao C L 2007 *J. Light-wave Technol.* **25** 3563
- [19] Xi X M, Chen Z L, Sun G L and Hou J 2011 *Appl. Opt.* **50** E50